JOURNAL OF MATERIALS SCIENCE 23 (1988) 919–923

Electrical conduction in non-metallic rare-earth solids

H. B. LAL, KANCHAN GAUR
Department of Physics, University of Gorakhpur, Gorakhpur 273009, India

Schematic energy band diagrams for the genesis of charge carriers in non-metallic rare-earth solids have been presented. It has been shown that positions of 4f bands have significant effect on the genesis and nature of charge carriers, their conduction mechanism and magnitude of electrical conductivity (σ) and Seebeck coefficient (S) of the solid. Relevant relations have been given for both σ and S in different situations. Experimental data on rare-earth sesquioxides (R_2O_3), rare-earth tungstates [$R_2(WO_4)_3$] and rare-earth molybdates [$R_2(MoO_4)_3$] in the intrinsic range have been explained as examples for the validity of energy band diagrams.

1. Introduction

The energy band model proposed more than fifty years ago has been quite successful in explaining the genesis of charge carriers in semiconductors and insulators. According to this model electrical conduction in non-metallic solids is governed by two broad bands: one completely filled at absolute zero called a valence band and the other completely empty at absolute zero called a conduction band. As temperature is raised electrons from the valence band are excited to the conduction band creating holes in the former. The holes and electrons conduct in their respective bands and give appreciable conductivity to the solid. We have seen that this simple model is capable of explaining electronic conduction in many rare-earth solids like their oxides, tungstates and molybdates. Rare-earth elements are characterized by the successive filling of 4f electronic shells, which lie inside 5s, 5p and 6s orbitals. The wave functions of 4f electrons do not have much spatial extension and do not overlap when rare-earth elements form solids. Thus 4f energy bands are extremely narrow (~ 0.05 eV) in most of the ionic rare-earth solids [1–4]. Such a narrow band cannot support band conduction. The only possible conduction is due to the hopping process which has extremely low mobility [5]. This is the reason why most of the rare-earth solids, although containing partially filled 4f bands, are non-metallic. It appears from the above discussion that 4f bands are not useful in electrical conduction. However, this is not the case. The relative position of this band has significant effect on the nature and mechanism of electronic conduction. This paper discusses how the position of localized $4f^n$ and excited $4f^{n+1}$ levels become effective in doing this.

2. Position of 4f bands and electrical conduction

We consider that relevant bands for the electrical conduction of a typical non-metallic rare-earth solid are the conduction band, valence band and extremely narrow $4f^n$ and $4f^{n+1}$ bands (or levels). Regarding the relative position of 4f bands we can have the following situations

(a) Both $4f^n$ and $4f^{n+1}$ bands lie outside the energy band gap.
(b) $4f^n$ band lies within the band gap and $4f^{n+1}$ lies outside the gap.
(c) $4f^{n+1}$ band lies within the band gap and $4f^n$ lies outside the gap.
(d) Both $4f^n$ and $4f^{n+1}$ bands lie within the energy band gap.

All these situations are schematically shown in Fig. 1.

Case (a): In this case 4f bands are not going to play any significant role. It is a simple case of a two broad energy band model discussed in normal text books. The electrical conductivity (σ) and Seebeck coefficient (S) are given by the following equations [6]

$$\sigma = \sigma_0 \exp(-E_g/2kT) \quad (1)$$

$$\sigma_0 = 2e\left(\frac{2\pi kT}{h^2}\right)^{3/2} (m_e^* m_h^*)^{3/4} (\mu_e + \mu_h) \quad (2)$$

$$S = \frac{E_g}{2e}\left(\frac{c-1}{c+1}\right)\frac{1}{T} + \frac{2k}{e}\left(\frac{c-1}{c+1}\right) + \frac{3k}{4e}\log_e a \quad (3)$$

where $a = m_e^*/m_h^*$, $c = \mu_e/\mu_h$, m_e^* and m_h^* and μ_e and μ_h are the effective masses and mobilities of electrons and holes respectively, E_g is the energy band gap of the solid and other symbols have their usual meaning. The plot of log σ against T^{-1} will be a straight line with a slope of $E_g/2$. Since temperature variations of μ_e and μ_h and m_e^* and m_h^* are similar in nature, it is reasonable to assume that their ratio will be fairly constant with temperature. Thus Equation 3 can be written as

$$S = \eta/eT + K_1 \quad (4)$$

where

$$\eta = \left(\frac{E_g}{2}\right)\left(\frac{c-1}{c+1}\right)$$

0022–2461/88 $03.00 + .12

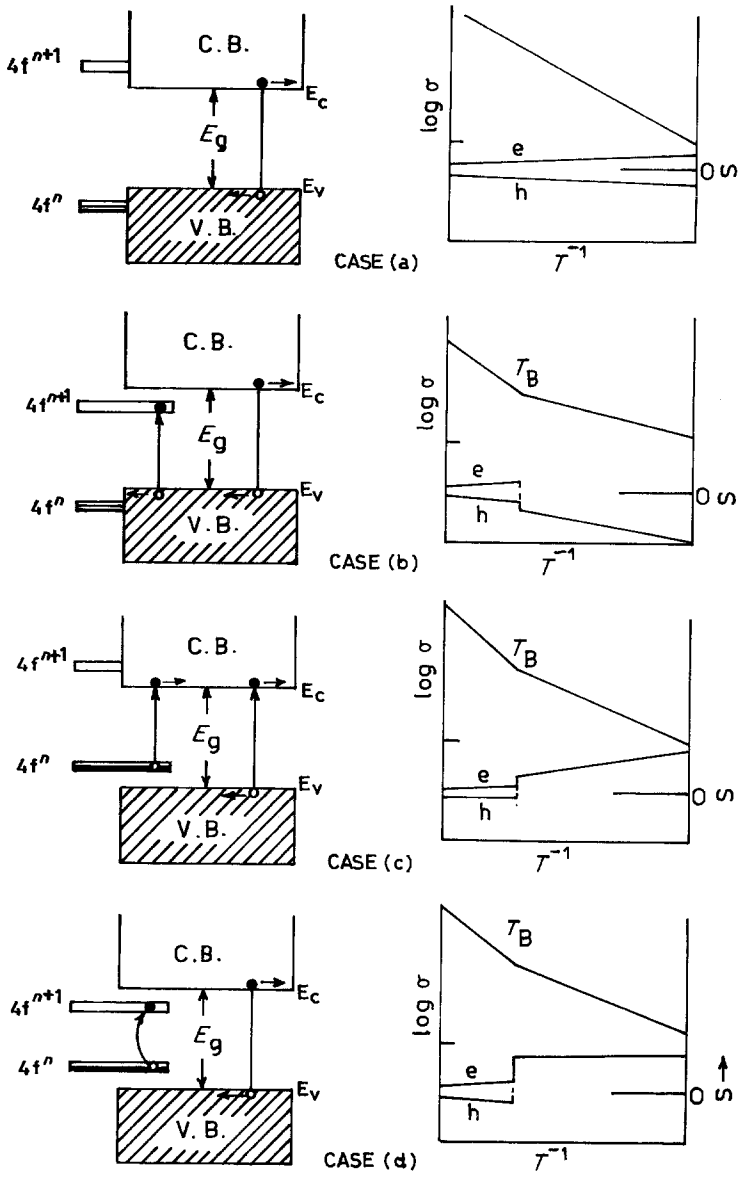

Figure 1 Energy band diagram and resulting electrical conductivity (σ) and Seebeck coefficient (S).

and

$$K_1 = \frac{2k}{e}\left(\frac{c-1}{c+1}\right) + \frac{3}{4}\frac{k}{e}\log_e a \qquad (5)$$

are constants. Thus the plot of S against T^{-1} will be a straight line with a slope η. Since electron and hole are both conducting in a relatively broad band giving $c \sim 1$, η will be very small in comparison to $E_g/2$ and K_1 will also be very small ($\sim$ few μV). Experimentally, variations of σ and S with T can be studied and the straight line plots stated above can be obtained for solids falling in this category. From these plots E_g, η, K_1 can be obtained and c and a can be calculated thereafter. Now taking a simplified assumption that $m_e^* = m_h^* = m$ (bare electron mass), the order of μ_e and μ_h can be estimated.

Case (b): In this case the favoured energy process for charge generation will be excitation of electrons from the $4f^n$ level to the conduction band. The holes thereby generated in the $4f^n$ level are almost localized and $\mu_e \gg \mu_h$. The variation of σ and S in this case will be given by the expression [7]

$$\sigma = A(T)\exp\left(-\frac{\lambda W}{2kT}\right) \qquad (6)$$

which for $m_h^* \gg m_e^*$ contains

$$A(T) = 2\left[\left(\frac{2\pi m_e^* kT}{h^2}\right)^{3/2} N\right]^{1/2} \mu_e e \qquad (7)$$

and

$$S = \left(\frac{W}{2e}\right)\frac{1}{T} + K_2 \qquad (8)$$

In the above equations $\lambda = 1$ for intrinsic conduction, N is the number of rare-earth ions per unit volume and K_2 is a constant. The charge carriers will be electrons. The plots of log σ and S against T^{-1} will be a straight line with almost the same slope. Here it is much easier to estimate μ_e, because N can be obtained from the density and structure of the compound and m_e^* can be taken as equal to m for this purpose. It must be mentioned that at much higher temperatures the conduction will be taken over by the charge carriers generated by the excitation of electrons from valence band to conduction band.

Case (c): In this case the favoured energy process for charge generation will be excitation of electrons from valence band to excited state $4f^{n+1}$ band. Advancing parallel argument as has been done for case (b), one

can express relations for σ and S as

$$\sigma = B(T) \exp\left(-\frac{\lambda W}{2kT}\right) \quad (9)$$

which for $m_e^* \gg m_h^*$ and $\mu_e \gg \mu_h$ has

$$B(T) = 2\left[\left(\frac{2\pi m_h^* kT}{h^2}\right)^{3/2} N\right]^{1/2} \mu_h e \quad (10)$$

provided the excitation to conduction band is neglected and

$$S = \left(\frac{W}{2e}\right)\frac{1}{T} + K_3 \quad (11)$$

where $\lambda \sim 1$, K_3 is a constant and other symbols have their usual meaning. The charge carriers will be holes. The plots of log σ and S against T^{-1} will be a straight line with almost the same slope. Here again it is easy to estimate μ_h from the experimental value of $B(T)$ if one can take $m_h^* = m$. At higher temperatures excitation of electrons from valence band to conduction band may become effective and conduction may be taken over by charge carriers generated by this process. The situation will then be governed by case (a).

Case (d): In this case electrical conduction will be due to hopping of electrons in the $4f^n$ band; which will behave as small polaron. The conductivity will be small. The Seebeck coefficient due to small polaron is very small and independent of temperature [5]. However, at a much higher temperature conduction will be taken over by the charge carriers generated by excitation of electrons from the valence to the conduction band.

3. Results for some common compounds and discussion

3.1. Rare-earth sesquioxides

Rare-earth sesquioxides (R_2O_3) are the most common compounds of the rare-earth elements. However, they have a variety of phases [8] namely hexagonal (A–type), monoclinic (B–type) and cubic (C–type). Some of the electrical transport properties of these compounds have been reported by us [9–15]. It has been found that intrinsic electronic conduction in these solids can be explained using energy band diagrams for the genesis of charge carriers and polaronic concepts for their conduction. The appropriate energy bands for electronic conduction in these solids are $R^{3+}:5d$, $R^{3+}:4f^n$, $O^{2-}:2p$ and $R^{2+}:4f^{n+1}$. High temperature magnetic susceptibility data on R_2O_3 [16] are compatible with $R^{3+}:4f^n$ configuration which indicates that $4f^n$ electrons are localized. Thus only $O^{2-}:2p$ and $R^{3+}:5d$ bands are relevant for electrical conduction. The former may be regarded as valence and the latter as conduction bands. The energy level diagram which explains the genesis of charge carriers in R_2O_3 is shown in Fig. 2. The position of $4f^n$ and $4f^{n+1}$ levels may change in different structures. According to this band diagram the electrical conduction process in La and Gd–Er should follow case (a), Sm, Eu, Tm and Yb should follow case (b) and Ce, Pr, Nd and Tb should follow case (c). The experimental results shown in Table I are in accordance with this prediction.

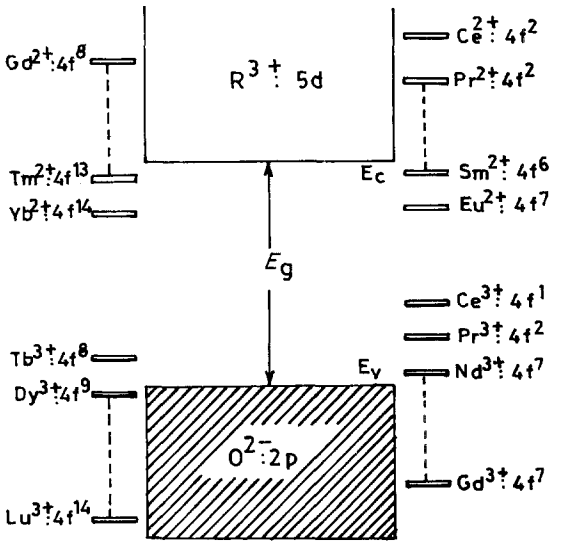

Figure 2 Energy band diagram for rare-earth sesquioxides.

3.2. Rare-earth tungstates

Rare-earth tungstates are another important compound of rare-earths. They also occur in a variety of structures [17]. Some of the magnetic and electrical

TABLE I Summarized results, their interpretation and mobilities of charge carriers in the intrinsic range of rare-earth sesquioxides [$\sigma = C^* \exp(-W/2kT)$, $S = \eta/et + H$]

R_2O_3 with R	Structure type	W (eV)	C* (Ω^{-1} m^{-1})	Temperature range (K)	η (eV)	H (mVK^{-1})	Charge† carrier	Case	W stands for	Mobility (cm^{-2} V^{-1} sec^{-1}) 900 K	
										μ_h	μ_e
La	A	2.40	2.40×10^3	700–1200	−0.05	−0.12	h	a	E_c–E_v	0.628	0.602
Nd	A	2.36	3.16×10^3	700–1200	–	–	e	b	E_c–$E(4f^3)$	–	0.188
Sm	B	2.12	2.68×10^2	800–1200	−0.50	−0.70	h	c	$E(4f^6)$–E_v	0.084	–
Eu	C	1.84	4.63×10^1	800–1200	–	–	h	c	$E(4f^7)$–E_v	0.327	–
Gd	B	2.44	8.75×10^2	800–1200	−0.30	−0.50	h	a	E_c–E_v	0.076	0.046
Gd	C	2.64	4.60×10^2	800–1200	−0.10	−0.30	h	a	E_c–E_v	0.126	0.117
Tb	B	2.24	3.08×10^7	750– 900	–	–	e	b	E_c–$E(4f^8)$	–	2.10
Dy	C	2.82	4.13×10^1	800–1200	−0.05	−0.15	h	a	E_c–E_v	0.011	0.010
Ho	C	2.74	5.13×10^2	800–1200	−0.05	−0.10	h	a	E_c–E_v	0.133	0.128
Er	C	3.04	1.66×10^3	800–1200	−0.10	−0.10	h	a	E_c–E_v	0.449	0.420
Tm	C	2.84	2.96×10^2	800–1200	−0.80	−0.70	h	c	$E(4f^{13})$–E_v	0.426	–
Yb	C	2.66	2.36×10^2	800–1200	−0.90	−0.60	h	c	$E(4f^{14})$–E_v	0.321	–

*C may stand for σ_0, $A(T)$ or $B(T)$ in different cases.
†Obtained on the basis of the sign of S.

TABLE II Summarized results, their interpretation and mobilities of charge carriers in the intrinsic range of rare-earth tungstates [$\sigma = C^* \exp(-W/2kT)$, $S = \eta/eT + H$]

$R_2(WO_4)_3$ with R	W (eV)	C* (Ω^{-1} m^{-1})	Temperature range (K)	η (eV)	H (mVK^{-1})	Charge† carrier	Case	W stands for	Mobility (cm^2 V^{-1} sec^{-1}) at 900 K	
									μ_e	μ_h
La	2.40	1.23×10^2	1050–1200	–	–	h	a	$E_c - E_v$	–	–
Ce	1.90	5.20×10^1	600– 800	0.10	−0.10	e	b	$E_c - E(4f^1)$	1.30	–
Pr	2.12	1.30×10^1	600– 950	0.80	−0.70	e	b	$E_c - E(4f^2)$	0.25	–
	2.48	1.06×10^2	1000–1200	–	–	h	a	$E_c - E_v$	–	–
Nd	2.50	2.60×10^3	1000–1200	−0.15	+0.01	h	a	$E_c - E_v$	0.60	0.86
Sm	2.00	6.50×10^1	600–1200	−0.60	±0.06	h	c	$E(4f)^6 - E_v$	–	1.25
Eu	1.84	2.35×10^2	600– 800	–	–	h	c	$E(4f^7) - E_v$	–	5.02

*C may stand for σ_0, A(T) or B(T) in different cases.
†Obtained on the basis of the sign of S.

properties of these compounds have been studied by us [18–21]. It has been found that electrical conduction in these solids can be explained using the energy band theory and the polaronic concept. The relevant bands for electrical conduction in these solids are filled O^{2-} : 2p, empty R^{3+} : 5d and W^{6+} : 5d and localized R^{3+} : $4f^n$ and $4f^{n+1}$ levels. The values of conductivity of rare-earth tungstates are of the same order as those of their sesquioxides [14]. Hence only bands relating to R^{3+} and O^{2-} need to be considered. The 5d orbitals at tetrahedral W^{6+} ions are completely ignored, they should be at higher energies than the R^{3+} : 5d band. Elimination of W^{6+} : 5d band leaves the relevant bands for electrical conduction to be the R^{3+} : 5d conduction band, the O^{2-} : 2p valence band and localized R^{3+} : $4f^n$ configuration. The schematic energy band diagram which explains the electrical conduction in these solids is shown in Fig. 3. It is clear from this band picture that the electrical conduction process in Ce, Pr and Tb tungstates should be according to case (a), Nd, Gd-Yb should follow case (b) and Sm and Eu tungstates case (c). The experimental results shown in Table II are in accordance with the above prediction.

3.3. Rare-earth molybdates

The interest in the study of rare-earth molybdates arose when some of them were recognized to possess ferroelectric and ferroelastic properties. We have studied magnetic and electrical transport properties [22–24] of these solids and have found that electrical conduction in these solids can be explained using the energy band model. It has been discussed [24] that relevant bands for electrical conduction in this class of solids are the Mo^{6+} : 4d conduction band and the O^{2-} : 2p valence band. The schematic energy band diagram for these solids is shown in Fig. 4. The experimental results of σ and S measurements together with the other relevant data obtained on the basis of the generalized case are given in Table III. The results are in accordance with the predictions of the energy band model.

It must be pointed out at this stage that due to the ionic nature of rare-earth compounds, there is a strong possibility of polaron formation. Thus the charge carrier for the conduction process will be electron or hole polarons. It has been discussed [10, 14, 21], that in many of these compounds the polaron

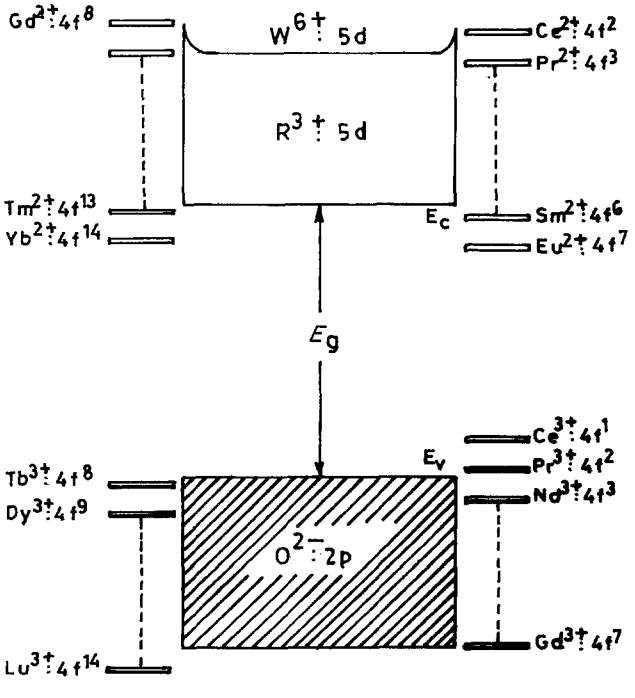

Figure 3 Energy band diagram for rare-earth tungstates.

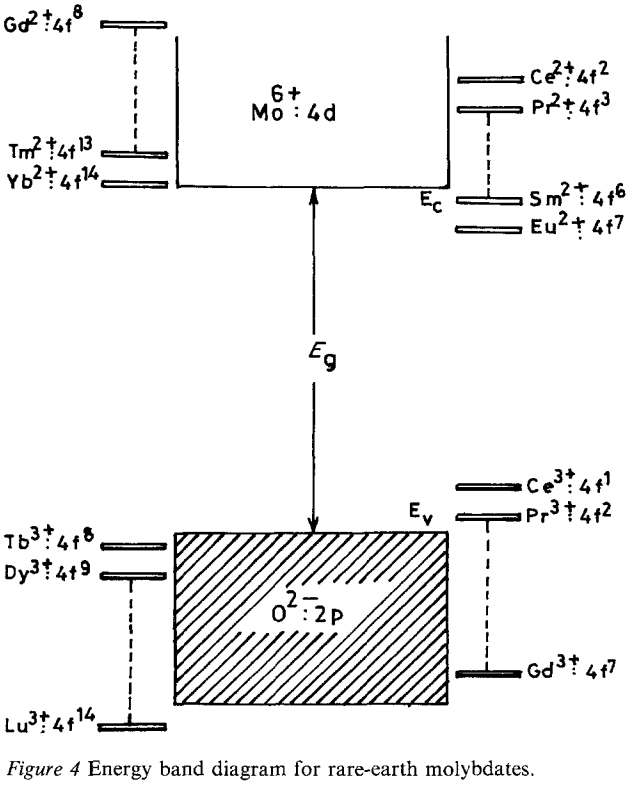

Figure 4 Energy band diagram for rare-earth molybdates.

TABLE III Summarized results, their interpretation and mobilities of charge carriers in the intrinsic range of rare-earth molybdates [$\sigma = C^* \exp(-W/2kT)$, $S = \eta/eT + H$]

$R_2(MoO_4)_3$ with R =	W (eV)	C* ($\Omega^{-1} m^{-1}$)	Temperature range (K)	η (eV)	H (mVK^{-1})	Charge† carrier	Case	W stands for	Mobility ($cm^2 V^{-1} sec^{-1}$) $\mu_e \simeq \mu_h$
Gd	3.40	5.05×10^2	900–1200	0.005	0.145	e	a	E_c-E_v	0.011
Tb	3.40	5.05×10^2	910–1200	0.005	0.095	e	a	E_c-E_v	0.011
Dy	3.50	8.10×10^4	920–1200	0.005	0.145	e	a	E_c-E_v	0.237
Ho	3.60	3.04×10^4	830–1200	0.005	0.145	e	a	E_c-E_v	0.187
Er	3.74	4.96×10^6	1000–1200	0.005	0.145	e	a	E_c-E_v	2.37
Tm	3.84	1.85×10^6	1000–1200	0.000	0.10	e	a	E_c-E_v	1.93
Yb	4.00	8.92×10^6	1000–1200	0.000	0.10	e	a	E_c-E_v	9.31

*C may stand for σ_0, $A(T)$ or $B(T)$ in different cases.
†Obtained on the basis of the sign of S.

formed are large polaron with intermediate coupling ($1 < \alpha < 6$). The mobility of charge carriers in such a case becomes

$$\mu = \mu_0 \exp(\hbar\omega_0/kT) \quad (12)$$

where ω_0 is the longitudinal optical mode frequency. The experimental observed slope of log σ against T^{-1} plot in such a case will correspond to an energy of $(E_g/2 + \hbar\omega_0)$ instead of E_g, and mobility will increase with increasing temperature.

Acknowledgement

One of the authors (KG) is thankful to CSIR for financial assistance.

References

1. Y. A. ROCHAR, *Adv. Phys.* **11** (1962) 233.
2. B. CONQBLIN and A. BLANDIN, *ibid.* **17** (1968) 28.
3. C. E. T. GONCALVES DASILVA and L. M. FALICOV, *J. Phys. C: Solid State Phys.* **5** (1972) 63.
4. R. RAMIREZ and L. M. FALICOV, *Phys. Rev.* **B3** (1971) 2425.
5. A. J. BOSMAN and H. J. VAN DAAL, *Adv. Phys.* **19** (1970) 1.
6. T. C. HERMAN and J. M. HONIG, "Thermoelectric and Thermomagnetic Effects and Applications", (McGraw Hill, New York 1967) 142.
7. G. C. JAIN and W. B. BERRY, "Transport Properties of Solid and Solid State Energy Conversion", (Tata McGraw Hill Publishing Company Ltd., Bombay, New Delhi 1972) p. 37.
8. G. BRAUER, "Progress in Science and Technology of Rare-Earths", edited by L. Eyring (Pergamon Press, Oxford 1966) 312.
9. H. B. LAL and N. DAR, *Indian J. Pure Appl. Phys.* **14** (1976) 788.
10. H. B. LAL, B. K. VERMA and N. DAR, *Indian J. Cryogenics* **1** (1976) 119.
11. H. B. LAL, V. PRATAP and N. DAR, *Indian J. Pure Appl. Phys.* **15** (1977) 366.
12. H. B. LAL, B. K. VERMA and N. K. SANYAL, *Proc. Natn. Acad. Sci. India* **47A** (1977) 1.
13. V. PRATAP, B. K. VERMA and H. B. LAL, *ibid.* **48A** (1978) 1.
14. B. K. VERMA, V. PRATAP and H. B. LAL, *Indian J. Pure Appl. Phys.* **18** (1980) 150.
15. H. B. LAL, *J. Phys. C: Solid State Phys.* **13** (1980) 3969.
16. H. B. LAL, V. PRATAP and A. KUMAR, *Pramana* **10** (1978) 409.
17. L. H. BRIXNER and A. W. SLEIGHT, *Mater. Res. Bull.* **8** (1973) 1269.
18. H. B. LAL and N. DAR, *J. Phys. Chem. Solids* **38** (1977) 161.
19. N. DAR and H. B. LAL, *Pramana* **11** (1978) 705.
20. *Idem, Mater. Res. Bull.* **14** (1979) 1263.
21. B. K. VERMA and H. B. LAL, *Mater. Res. Bull.* **16** (1981) 1579.
22. V. PRATAP and H. B. LAL, *Natn. Acad. Sci. Lett.* **1** (1978) 38.
23. A. K. TRIPATHI and H. B. LAL, *J. Phys. Soc. Jpn* **49** (1980) 1896.
24. V. PRATAP, K. GAUR and H. B. LAL, *Mater. Res. Bull.* **22** (1987) 1381.

Received 6 April
and accepted 10 July 1987